

Broadband third-order optical nonlinearities of layered franckeite towards mid-infrared regime

Zhi-Qiang Xu(徐志强), Tian-Tian Zhou(周甜甜), Jie Li(李洁), Dong-Yang Liu(刘东阳), Yuan He(何源), Ning Li(李宁), Xiao Liu(刘潇), Li-Li Miao(缪丽丽), Chu-Jun Zhao(赵楚军), and Shuang-Chun Wen(文双春)

Citation: Chin. Phys. B, 2024, 33 (**10**): 104208. DOI: 10.1088/1674-1056/ad6ccb
Journal homepage: http://cpb.iphy.ac.cn; http://iopscience.iop.org/cpb

What follows is a list of articles you may be interested in

Surface phonon resonance: A new mechanism for enhancing photonic spin Hall effect and refractive index sensor

Jie Cheng(程杰), Chenglong Wang(汪承龙), Yiming Li(李一铭), Yalin Zhang(张亚林), Shengli Liu(刘胜利), and Peng Dong(董鹏)
Chin. Phys. B, 2024, 33 (**8**): 084201. DOI: 10.1088/1674-1056/ad4a3c

Tailoring topological corner states in photonic crystals by near- and far-field coupling effects

Zhao-Jian Zhang(张兆健), Zhi-Hao Lan(兰智豪), Huan Chen(陈欢), Yang Yu(于洋), and Jun-Bo Yang(杨俊波)
Chin. Phys. B, 2023, 32 (**12**): 124201. DOI: 10.1088/1674-1056/acddd3

A 3-5 μm broadband YBCO high-temperature superconducting photonic crystal

Gang Liu(刘刚), Yuanhang Li(李远航), Baonan Jia(贾宝楠), Yongpan Gao(高永潘), Lihong Han(韩利红), Pengfei Lu(芦鹏飞), and Haizhi Song(宋海智)
Chin. Phys. B, 2023, 32 (**3**): 034213. DOI: 10.1088/1674-1056/acb760

Mid-infrared lightly Er^{3+}-doped CaF^{2} laser under acousto-optical modulation

Yuan-Hao Zhao(赵元昊), Meng-Yu Zong(宗梦雨), Jia-Hao Dong(董佳昊), Zhen Zhang(张振), Jing-Jing Liu(刘晶晶), Jie Liu(刘杰), and Liang-Bi Su(苏良碧)
Chin. Phys. B, 2023, 32 (**3**): 034203. DOI: 10.1088/1674-1056/aca4c0

Generation of mid-infrared supercontinuum by designing circular photonic crystal fiber

Ying Huang(黄颖), Hua Yang(杨华), and Yucheng Mao(毛雨澄)
Chin. Phys. B, 2022, 31 (**5**): 054211. DOI: 10.1088/1674-1056/ac272c

---

Broadband third-order optical nonlinearities of layered franckeite towards mid-infrared regime

Zhi-Qiang Xu(徐志强)[1], Tian-Tian Zhou(周甜甜)[1], Jie Li(李洁)[2], Dong-Yang Liu(刘东阳)[1], Yuan He(何源)[1], Ning Li(李宁)[1], Xiao Liu(刘潇)[1], Li-Li Miao(缪丽丽)[1,†], Chu-Jun Zhao(赵楚军)[1], and Shuang-Chun Wen(文双春)[1]

[1] *Key Laboratory for Micro/Nano Optoelectronic Devices of Ministry of Education & Hunan Provincial Key Laboratory of Low-Dimensional Structural Physics and Devices, School of Physics and Electronics, Hunan University, Changsha* 410082, *China*

[2] *School of Mechanical and Electrical Engineering, Heze University, Heze* 274015, *China*

(Received 18 June 2024; revised manuscript received 15 July 2024; accepted manuscript online 8 August 2024)

The study of nonlinear optical responses in the mid-infrared (mid-IR) regime is essential for advancing ultrafast mid-IR laser applications. However, nonlinear optical effects under mid-IR excitation are rarely reported due to the lack of suitable nonlinear optical materials. The natural van der Waals heterostructure franckeite, known for its narrow bandgap and stability in air, shows great potential for developing mid-IR nonlinear optical devices. We have experimentally demonstrated that layered franckeite exhibits a broadband wavelength-dependent nonlinear optical response in the mid-IR spectral region. Franckeite nanosheets were prepared using a liquid-phase exfoliation method, and their nonlinear optical response was characterized in the spectral range of 3000 nm to 5000 nm. The franckeite nanosheets exhibit broadband wavelength-dependent third-order nonlinearities, with nonlinear absorption and refraction coefficients estimated to be about 10^{-7} cm/W and 10^{-11} cm^2/W, respectively. Additionally, a passively Q-switched fluoride fiber laser operating around a wavelength of 2800 nm was achieved, delivering nanosecond pulses with a signal-to-noise ratio of 43.6 dB, based on the nonlinear response of franckeite. These findings indicate that layered franckeite possesses broadband nonlinear optical characteristics in the mid-IR region, potentially enabling new possibilities for mid-IR photonic devices.

Keywords: third-order optical nonlinearities, franckeite, mid-infrared, Q-switching

PACS: 42.65.–k, 42.65.Re, 42.55.Wd, 42.70.Nq **DOI:** 10.1088/1674-1056/ad6ccb

1. Introduction

Mid-infrared (mid-IR) lasers have garnered significant attention in recent years due to their extensive applications in various fields such as environmental monitoring, medical diagnostics, and chemical sensing. On the other hand, mid-IR optical materials are crucial for developing advanced photonic devices. When combined with mid-IR lasers, lasers can produce coherent light in the mid-IR range, which is highly beneficial for applications requiring precise and powerful light sources. The development of mid-IR optical materials and fiber lasers involves overcoming significant technical challenges, including the need for materials with suitable transparency, durability, and nonlinearity. Although some preliminary research and exploration have been conducted on optical materials in the mid-IR spectrum,[1–7] researchers are still striving to find stable mid-IR optical materials with broadband nonlinear responses.

Franckeite, a naturally occurring van der Waals (vdWs) heterostructure, is the first naturally occurring quasi two-dimensional (2D) vdWs heterostructure exfoliated from bulk form composed of alternating SnS_2-like and PbS-like layers. In comparison with the artificial vdWs heterostructures, franckeite-based vdWs heterostructures feature a desirable narrow bandgap and air stability, making it well-suited for wide-band photoresponse and optoelectronic applications.[8–10] Although franckeite is composed of a sequence of isotropic 2D layers, it exhibits optical in-plane anisotropy.[11] The effect of the crystal structural anisotropy on the nonlinear harmonic generation in naturally occurring 2D heterostructure has also been explored.[12–16] In addition, the layered franckeite exhibits a broadband nonlinear optical response and ultrafast carrier dynamics in the near-infrared wavelengths.[17,18] Franckeite also displays a strong topological character with high concentration in both three-dimensional and few-layered forms, with unique electronic properties that are stable.[19] Recent progress on franckeite nanosheets highlight their potential as suitable candidate for broadband nanophotonic devices.[20–24]

Accompany with broadband nonlinear optical properties, franckeite has seen considerable study in its applications within lasers. Passive mode-locked ytterbium- and erbium-doped fiber laser has been proposed using franckeite-based saturation absorption (SA) as modulator.[25,26] The electronic transport measurements indicate that franckeite is a p-doped semiconductor with a mid-/far-infrared band gap.[8] Despite

†Corresponding author. E-mail: lilimiao@hnu.edu.cn

© 2024 Chinese Physical Society and IOP Publishing Ltd

this, its exploration in the mid-IR range remains limited, highlighting a gap in the exploration of these materials' potential. Exploration of nonlinear optical response in the mid-IR region, is highly desirable for ultrafast mid-IR tunable coherent laser sources.[27] This work seeks to underscore the need for expanded research into franckeite, particularly in the underexplored mid-infrared region, which could unlock new avenues for optoelectronic applications.

Here, the naturally occurring vdWs heterostructure franckeite has been demonstrated to exhibit a wavelength-dependent broadband nonlinear optical response in the mid-IR spectral region. The layered franckeite was prepared through liquid-phase exfoliation method. Furthermore, their nonlinear optical behavior was investigated by *Z*-scan technique where both open and closed aperture measurements were performed. Further, it is utilized as a saturable absorber in fluoride fiber lasers. These results showed that the layered franckeite has the excellent third-order nonlinear characteristics in mid-IR regime, which can broaden the range of applications for mid-IR photonics.

2. Preparation and characterization

The process of liquid-phase exfoliation of natural occurring vdWs superlattices introduces a novel method for creating ultrathin, air-stable, and clean vdWs heterostructures with correct lattice alignments.[8] In this study, the franckeite, from Marin Mineral Company, was processed by liquid-phase exfoliation method. Initially, the solid franckeite was pulverized into powder form using a pestle and mortar, then dispersed in an N-methyl-2-pyrrolidone organic solvent, which can help promote layer separation and the stabilization of nanosheets.[9] Following ultrasonic treatment for two hours at a water bath temperature of 22 °C, the mixture was centrifuged at 5000 rpm for 10 min. Afterwards, the supernatant was then spin-coated onto quartz glass substrates to fabricate nanosheets for further experimental investigation. The thickness measurement of the layered franckeite film, conducted using an atomic force microscope, is presented in Fig. 1(a). The cross-sectional view chosen for measurement, as illustrated in Fig. 1(c), reveals a height difference of approximately 7.7 nm between the substrate and the selected cross-section. Considering previous reports that the thickness of a franckeite monolayer is around 1.7 nm,[9] it suggests that the film consists of approximately five layers. The energy dispersive x-ray spectroscopy diagram, depicted in Fig. 1(b), delineates the elemental composition of the material. Sulfur is the predominant element, comprising 48.59% of the material, succeeded by lead with a 29.37% share, tin contributing 14.11%, and antimony making up approximately 7.92%, which is also consistent with the previous results.[8] The linear optical transmission spectrum from 900 nm to 2700 nm was assessed by an UV-VIS-NIR spectrophotometer (UV-3600PLUS, Shimadzu), revealing broadband absorption in the near-infrared to mid-IR bands, as shown in Fig. 1(d).

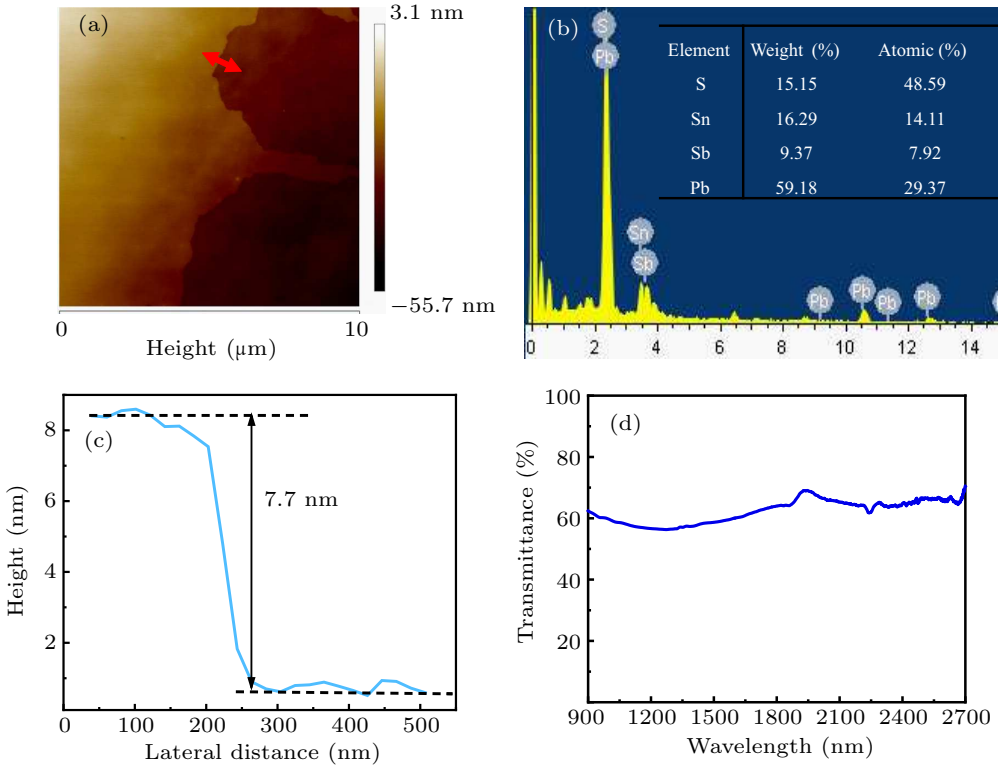


Fig. 1. Characterization of layered franckeite. (a) 2D atomic force microscope image. (b) Energy dispersive x-ray spectroscopy quantification and its atomic proportions of bulk franckeite. (c) The height profile marked from panel (a). (d) The linear absorbance spectrum of few-layer franckeite.

3. Results and discussion

3.1. Nonlinear optical response of layered franckeite

To explore the broadband optical nonlinearity of franckeite, both open-aperture (OA) and close-aperture (CA) *Z*-scan techniques are employed within femtosecond time domains. A femtosecond Ti:sapphire laser, with an optical parametric amplifier, facilitates the continuous tuning of the central wavelength across a broad spectrum. The pulse laser utilized in this study was femtosecond ultra-short pulse (Astrella Tunable-V-USP-1k, Coherent), which operates across a wavelength range of 3000 nm to 5000 nm, delivering pulses with a width of about 35 fs at a repetition rate of 1 kHz.

A typical *Z*-scan experimental setup, as illustrated in Fig. 2(a), includes a laser source, optical power attenuator, beam splitter, focusing lens, high-precision motorized translation stage, detectors, and data processing system. The incident laser beam first passed through a continuously adjustable optical power attenuator. The laser beam was then divided into two parts by a 1:9 optical beam splitter. One part was recorded by a thermopile detector (818P-001-12, Newport) and a power meter (Newport 2936) for reference. The other part was focused onto the sample by an optical convex lens with a focal length of 50 mm, resulting in a beam spot size of 80 μm at the focal point. The sample was mounted on a computer-controlled motorized translation stage. The transmittance of the sample through an aperture was monitored in the far field as a function of the sample's position. Additionally, the transmittance of the sample without the aperture was recorded. This allows for simultaneous OA and CA measurements. All measurements were conducted using CaF_2 lenses. By analyzing the experimental data, the nonlinear optical parameters of the material can be extracted.

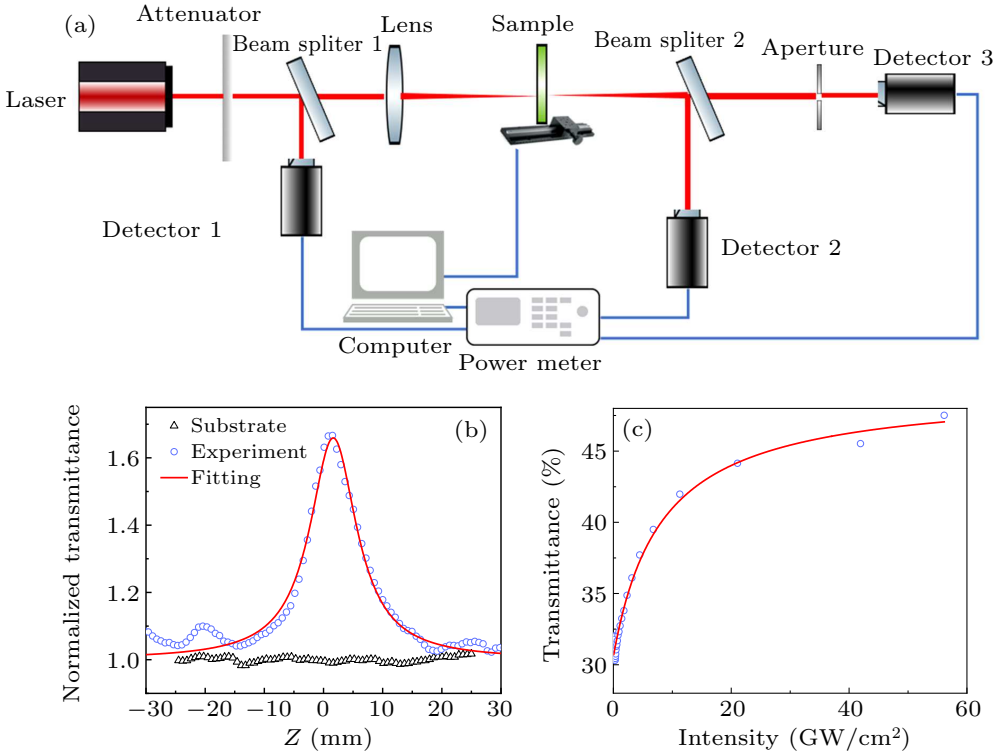


Fig. 2. Schematic diagram of the *Z*-scan setup and the saturation absorption characteristics of franckeite at 3000-nm wavelength. The solid line represents the fitting of the experimental data. (a) The *Z*-scan experimental setup, (b) the *Z*-scan measurement, and (c) the dependence of transmittance on input intensity for franckeite.

Figure 2(b) displays the OA results for layered franckeite with an incident pulse intensity of 134 GW/cm^2 at a wavelength of 3000 nm. The presence of a symmetrical peak at the focal point suggests an increase in light transmittance as the laser beam intensity grows when the sample approaches the focal point, attributable to the SA effect of the layered franckeite. It is obvious that the nonlinear optical effect of the substrate was negligible in comparison with the franckeite. To quantitatively evaluate the nonlinear absorption coefficients of the layered franckeite, these coefficients can be determined by fitting the data with the following expression:[28,29]

$$T(z) = 1 - \frac{\beta I_0 L_{\text{eff}}}{2\sqrt{2}(1+z^2/z_0^2)}, \tag{1}$$

where I_0 is the pump intensity at the focus, L_{eff} is the sample's effective length, and z_0 is the Rayleigh length. The nonlinear absorption coefficient is fitted to be -2.43×10^{-7} cm/W. Moreover, we plot the relationship between nonlinear transmission and incident laser intensity, as illustrated in Fig. 2(c). These curves align closely with an SA model predicated on one-photon absorption, and we can convert the positional co-

ordinate axis variable into a light intensity variable to obtain the trend of the franckeite's transmittance with light intensity I by the relationship as[30]

$$T = 1 - \left(\frac{a_s}{1 + I/I_{sat}} + a_{ns} \right), \tag{2}$$

where a_s is the modulation depth, and a_{ns} signifies the unsaturated component, while I_{sat} is the saturated light intensity. As depicted in Fig. 2(c), it is observed that as the light intensity escalates, the transmittance through franckeite steadily increases and then levels off, indicating that the material's absorption gradually approaches saturation, demonstrating its potential use as a saturable absorber. The extracted modulation depth, saturation intensity, and unsaturable loss are $\sim 17.6\%$, 10.2 GW/cm^2, and 34.9%, respectively.

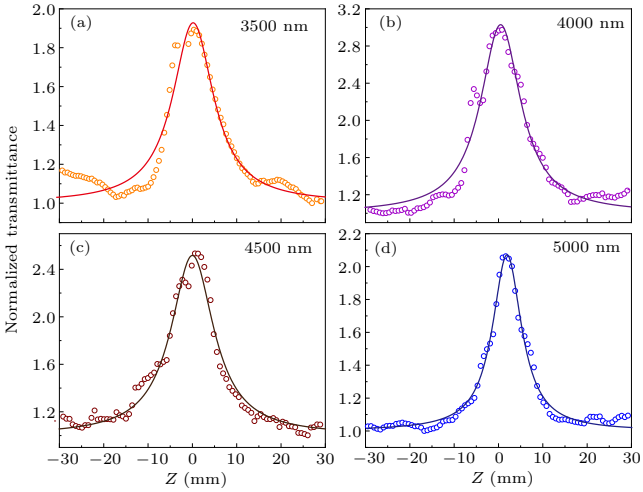


Fig. 3. The open-aperture Z-scan curves obtained at wavelengths of (a) 3500 nm, (b) 4000 nm, (c) 4500 nm, and (d) 5000 nm, respectively. The solid lines show the fit to the experimental data.

To verify the broadband nonlinear optics responses of franckeite, Z-scan technique was used to characterize the franckeite in the mid-IR band, which ranges from 3000 nm to 5000 nm. Figure 3 clearly shows that the normalized transmittance gradually increases and then decreases on both sides of the focal point for OA Z-scan. This behavior arises from the optical SA characteristics of franckeite. We fitted the nonlinear absorption coefficients of the three bands with incident intensity of 134 GW/cm^2, and the estimated nonlinear absorption coefficients are approximately -3.42×10^{-7} cm/W (at 3500 nm), -7.48×10^{-7} cm/W (at 4000 nm), -4.41×10^{-7} cm/W (at 4500 nm), and -3.15×10^{-7} cm/W (at 5000 nm) respectively. The negative sign of the coefficient indicates that the broadband saturated absorption characteristics of layered franckeite.

Correspondingly, CA Z-scan measurement was used to investigate the nonlinear refractive properties of franckeite. Figure 4 illustrates that typical peak-valley profile Z-scan curves can be achieved for all wavelengths. The general pattern of the curve involves an increase followed by a decrease in transmittance as the sample approaches and then moves past the focal point. The results indicate that franckeite is a self-defocusing medium, the nonlinear refractive index of franckeite in the mid-infrared band is -1.97×10^{-11} cm^2/W (at 3500 nm), -1.19×10^{-11} cm^2/W (at 4000 nm), -2.81×10^{-11} cm^2/W (at 4500 nm), -0.88×10^{-11} cm^2/W (at 5000 nm), respectively. The wavelength-dependent nonlinear absorption coefficient and nonlinear refractive index in franckeite was then analyzed, similar to graphene, the nonlinear response is dispersionless over the wavelength range in our experiments.[31] This may be attributed to the material's unique electronic structure, further demonstrating the stability of franckeite, which is promising for application where a constant response is important, for example, in such mid-IR robust nonlinear devices as optical limiters and switchable elements.

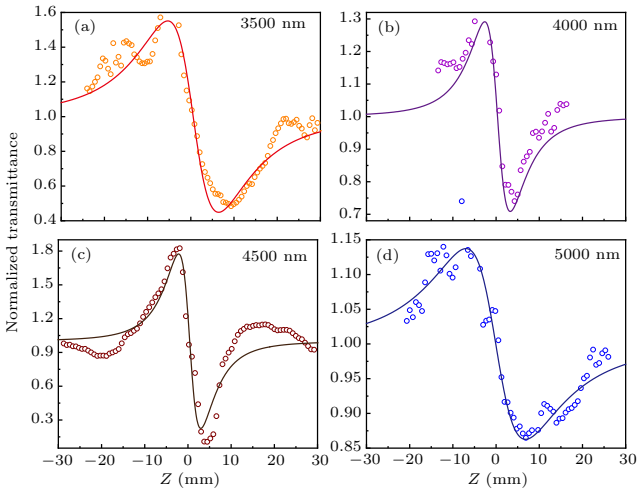


Fig. 4. The close-aperture Z-scan curves obtained at wavelengths of (a) 3500 nm, (b) 4000 nm, (c) 4500 nm, and (d) 5000 nm, respectively. The solid lines show the fit to the experimental data.

Table 1 presents the nonlinear optical responses of several typical 2D materials and heterojunctions.[32–43] Compared with artificial van der Waals heterostructures and 2D materials, the layered franckeite exhibits competitive nonlinear optical response, which indicates that franckeite is a potential nonlinear medium. In addition, previous studies on 2D materials and heterostructures have primarily focused on the near-infrared spectrum with the well-developed near-infrared light sources and optical devices. Despite the research conducted on mid-infrared optical materials,[41–43] mid-IR optical materials still face challenges such as stability and strong nonlinear responses to fully exploit their potential in various applications. The results for broadband nonlinear optical effects of the layered franckeite can develop mid-infrared nonlinear optical responses of layered materials and expand their applications.

Table 1. Comparisons of nonlinear optical parameters of typical heterojunctions and 2D materials.

Sample	λ (nm)	β (cm/W)	n_2 (cm^2/W)	References
hBN-GO	532	$\sim 1.34\times10^{-8}$	2.58×10^{-13}	[32]
Ag/MoS_2	532	3.5×10^{-4}	6.5×10^{-7}	[33]
GaN/AlGaN/GaN	–	-3.37×10^{-12}	-2.25×10^{-7}	[34]
Al_2O_3/ZnO	800	1.39×10^{-6}	7.43×10^{-11}	[35]
Bi_2S_3/MoS_2	800	-1.30×10^{-7}	–	[36]
InSe/graphene	1030	-5.81×10^{-7}	–	[37]
MoS_2/BP/ MoS_2	1550	-7.30×10^{-10}	-3.04×10^{-18}	[38]
Bi_2O_2Se	1550	-6.48×10^{-7}	$\sim 2.03\times10^{-11}$	[39]
GaAs	1680	$\sim 2.5\times10^{-10}$	$\sim 3\times10^{-13}$	[40]
BP	2100	$\sim -5.7\times10^{-11}$	–	[41]
Graphene	2400	-1.90×10^{-5}	-2.50×10^{-9}	[42]
CdO	2500	$\sim -3.7\times10^{-7}$	–	[43]
Franckeite	3000	-2.43×10^{-7}	-1.20×10^{-11}	this work
	3500	-3.42×10^{-7}	-1.97×10^{-11}	
	4000	-7.48×10^{-7}	-1.19×10^{-11}	
	4500	-4.41×10^{-7}	-2.81×10^{-11}	
	5000	-3.15×10^{-7}	-0.88×10^{-11}	

4. Mid-IR passively *Q*-switched Er^{3+}:ZBLAN fiber laser with franckeite

Motivated by the broadband saturable absorption and substantial modulation depth by franckeite in the mid-IR band, a passively *Q*-switched Er^{3+}:ZBLAN fiber laser incorporating franckeite-based saturable absorber was developed, the experimental setup can be found as previously shown.[44] Steadily *Q*-switched pulse was not observed until the incident pump power reached 0.5 W. Figure 5 summarizes the characteristics of the *Q*-switched operation of the fiber laser modulated by franckeite at an incident pump power of 1.58 W. In Fig. 5(a), multiple pulse trains were measured at different time scales of 1 ms, 200 μs, and 50 μs, demonstrating that the peak pulse intensity remained stable and nearly unchanged, indicating excellent stability of the pulsed laser. The narrowest pulse width recorded was 577 ns, as shown in Fig. 5(b). The output optical spectrum, depicted in Fig. 5(c), shows the laser's central wavelength at 2791 nm. Figure 5(d) illustrates the frequency spectrum with a center frequency of 98 kHz and a resolution of 15 Hz, revealing a signal-to-noise ratio of 43.6 dB. These findings indicate that the *Q*-switched fiber laser using franckeite demonstrates great stability.

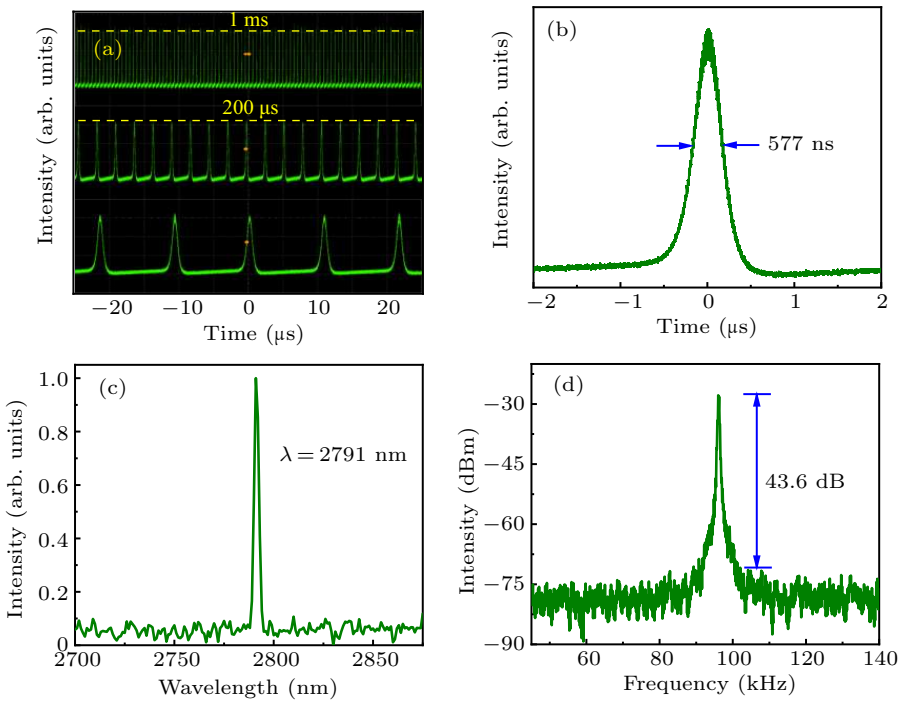


Fig. 5. Output characteristics of Er^{3+}:ZBLAN *Q*-switched fiber laser based on franckeite. (a) Pulse trains with different spans, (b) the single pulse of the laser, (c) optical spectrum, and (d) frequency spectrum.

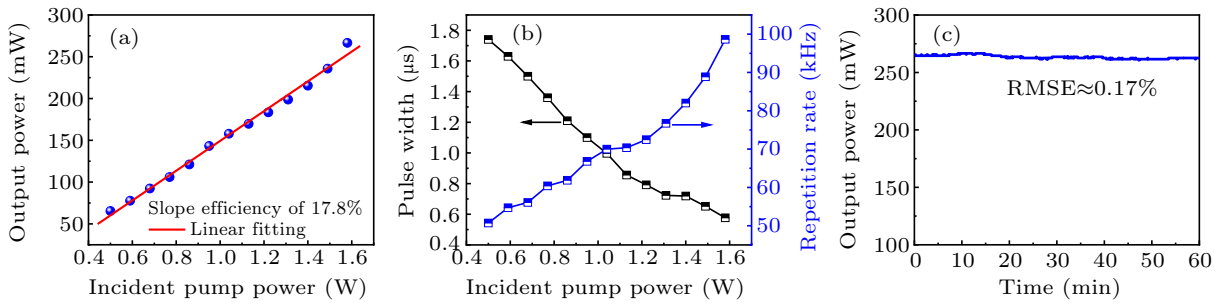


Fig. 6. (a) The relationship between the output power and the pump power; (b) the relationship between pulse width, pulse repetition rate, and varying pump power; and (c) the variation of the average output power of the pulse within 1 hour.

The relationship between the output power and the incident pump power is illustrated in Fig. 6(a). By varying the incident power from 0.5 W up to 1.58 W, the average pulse output power increased from 65.4 mW to 266.6 mW. This demonstrates that different power levels can be achieved in a stable Q-switching state with a slope efficiency of 17.8%. The linear relationship indicates the laser's excellent power scaling capability. Figure 6(b) shows the relationship between both pulse width and pulse repetition rate with the incident pump power. As the pump power increases, the pulse width steadily decreases and the pulse repetition rate increases, consistent with typical passively Q-switched lasers. The shortest pulse duration obtained was 577 ns at a frequency of 98.6 kHz, with an incident pump power of 1.58 W. In Fig. 6(c), the variation of the pulsed laser's output power over time at maximum output power was measured. Over a one-hour period, the fluctuation (root-mean-square error, RMSE) of the output power was approximately 0.17%. This low fluctuation indicates good long-term stability of the laser. These experimental results strongly suggest that franckeite is a promising candidate for broadband mid-infrared photonics and optoelectronics devices.

5. Conclusion

In conclusion, we have demonstrated that layered franckeite exhibits a broadband nonlinear optical response in the mid-IR spectral region. We study the third-order optical nonlinear response by Z-scan method with nonlinear absorption and refraction coefficients are estimated to be on the order of 10^{-7} cm/W and 10^{-11} cm^2/W, respectively. Based on the broadband nonlinear response and the stability of franckeite, an Er^{3+}:ZBLAN-doped fiber laser produces laser pulses as short as 577 ns, with a peak output power of 266.6 mW and a maximum pulse repetition rate of 98.6 kHz. The results can not only highlight franckeite's remarkable nonlinear optical characteristics in the mid-infrared spectrum but also underscore its applicability in mid-infrared modulator devices.

Acknowledgements

Project supported by the National Natural Science Foundation of China (Grant No. 61975055), the Natural Science Foundation of Hunan Province, China (Grant No. 2023JJ30165), the Natural Science Foundation of Shandong Province, China (Grant No. ZR2022QF005), and the Doctoral Fund of University of Heze (Grant No. XY22BS14).

References

[1] Chen X L, Lu X B, Deng B C, Sinai O, Shao Y C, Li C, Yuan S F, Tran V, Watanabe K, Taniguchi T, Naveh D, Yang L and Xia F N 2017 *Nat. Commun.* **8** 1672
[2] Zhu C H, Wang F Q, Meng Y F, Yuan X, Xiu F X, Luo H Y, Wang Y Z, Li J F, Lv X J. He L, Xu Y B, Liu J F, Zhang C, Shi Y, Zhang R and Zhu S N 2017 *Nat. Commun.* **8** 14111
[3] Ma J, Qin Z P, Xie G Q, Qian L J and Tang D Y 2019 *Appl. Phys. Rev.* **6** 021317
[4] Li J F, Luo H Y, Wang L L, Zhao C J, Zhang H, Li H P and Liu Y 2015 *Opt. Lett.* **40** 3659
[5] Guo Q B, Qin Z P, Wang Z, Weng Y X, Liu X F, Xie G Q and Qiu J R 2018 *ACS Nano* **12** 12770
[6] Liu S D, Jin Y C, Lv J W, Li K, Dong L L, Wang P F, Liu J T, Lu J P, Ni Z H and Zhang B T 2024 *Appl. Phys. Lett.* **124** 213101
[7] Liu J T, Yang F, Lu J P, Ye S, Guo H W, Nie H K, Zhang J L, He J L, Zhang B T and Ni Z H 2022 *Nat. Commun.* **13** 3855
[8] Velický M, Toth P S, Rakowski A M, Rooney A P, Kozikov A, Woods C R, Mishchenko A, Fumagalli L, Yin J, Zólyomi V, Georgiou T, Haigh S J, Novoselov K S and Dryfe R A W 2017 *Nat. Commun.* **8** 14410
[9] Molina-Mendoza A J, Giovanelli E, Paz W S, Nino M A, Island J O, Evangeli C, Aballe L, Foerster M, van der Zant H S J, Rubio-Bollinger G, Agrait N, Palacios J J, Perez E M and Castellanos-Gomez A 2017 *Nat. Commun.* **8** 14409
[10] Ray K, Yore A E, Mou T, Jha S, Smithe K K H, Wang B, Pop E and Newaz A K M 2017 *ACS Nano* **11** 6024
[11] Frisenda R, Sanchez-Santolino G, Papadopoulos N, Urban J, Baranowski M, Surrente A, Maude D K, Garcia-Hernandez M, van der Zant H S J, Plochocka P, San-Jose P and Castellanos-Gomez A 2020 *Nano Lett.* **20** 1141
[12] Dasgupta A, Gao J and Yang X D 2021 *npj 2D Mater. Appl.* **5** 74
[13] Dasgupta A, Gao J and Yang X D 2021 *Adv. Mater. Interfaces* **8** 2101106
[14] Dasgupta A, Yang X D and Gao J 2021 *npj 2D Mater. Appl.* **5** 88
[15] Tripathi R P N, Gao J and Yang X D 2021 *Sci. Rep.* **11** 8510
[16] Tripathi R P N, Yang X D and Gao J 2021 *Sci. Rep.* **11** 21895
[17] Li J, Du L, Huang J, He Y, Yi J, Miao L L, Zhao C J and Wen S C 2020 *Nanophotonics* **10** 927
[18] Li J, Yang K, Du L, Yi J, Huang J, Zhang J R, He Y, Huang B, Miao L L, Zhao C J and Wen S C 2020 *Adv. Opt. Mater.* **8** 2000382
[19] Paz W S, Menezes M G, Batista N N, Sanchez-Santolino G, Velický M, Varela M, Capaz R B and Palacios J J 2021 *Nano Lett.* **21** 7781
[20] Padilha J E, Fazzio A and da Silva A J R 2015 *Phys. Rev. Lett.* **114** 066803

[21] Burzurí E, Vera-Hidalgo M, Giovanelli E, Villalva J, Castellanos-Gomez A and Pérez E M 2018 *Nanoscale* **10** 7966
[22] Gusmão R, Sofer Z, Luxa J and Pumera M 2018 *J. Mater. Chem. A* **6** 16590
[23] Gan S W, Zhao Y T, Dai X Y and Xiang Y J 2019 *Results Phys.* **13** 102320
[24] Karki B, Sharma S, Singh Y and Pal A 2021 *Plasmonics* **17** 71
[25] Zhao H X, Li P, Li M, Xu L W, Hu Q Y, Zhang B, Liu J and Chen X H 2022 *Opt. Mater. Express* **12** 2844
[26] Xu Z R, Xu Z Q, Li N and Zhao C J 2023 *Results Phys.* **49** 106492
[27] Yi H H, Yao Y L, Zhang X and Ma G L 2023 *Chin. Phys. B* **32** 100509
[28] Sheik-Bahae M, Said A A, Wei T H, Hagan D J and Van Stryland E W V 1990 *IEEE J. Quantum Electron.* **26** 760
[29] Song M M, Huang Y F, Hao R X, Dong J H, Wu W S, Fu Z, Sa B S, Pei J J, Zheng J Y and Zhan H B 2022 *Appl. Surf. Sci.* **593** 153333
[30] Wu K, Chen B H, Zhang X Y, Zhang S F, Guo C S, Li C, Xiao P S, Wang J, Zhou L J, Zou W W and Chen J P 2018 *Opt. Commun.* **406** 214
[31] Hendry E, Hale P J, Moger J, Savchenko A K and Mikhailov S A 2010 *Phys. Rev. Lett.* **105** 097401
[32] Biswas S, Tiwary C S, Vinod S, Kole A K, Chatterjee U, Kumbhakar P and Ajayan P M 2017 *Phys. Chem. C* **121** 8060
[33] Ebrahimzadeh M, Haghighatzadeh A and Dutta J 2021 *Opt. Laser Technol.* **140** 107092
[34] Chen P, Zuo Y H, Tu X G, Cai D J, Li S P, Kang J Y, Yu Y D, Yu J Z and Wang Q M 2008 *Appl. Phys. Lett.* **92** 161112
[35] Can-Uc B, López J, Lizarraga-Medina E G, Borbon-Nuñez H A, Rangel-Rojo R, Marquez H, Tiznado H, Jurado-González J A and Hirata-Flores G 2019 *Opt. Express* **27** 17359
[36] Yang D, Lu C H, Ma J Y, Luo M W, Zhao Q Y, Jin Y P and Xu X L 2021 *Appl. Suf. Sci.* **538** 147989
[37] Lv H Y, Chu L R, Sun X L and Chen F 2023 *Mater. Lett.* **349** 134839
[38] Xiao S, Wang H, Qin Y L, Li X Q, Xin H, Wang G, Hu L, Wang Y W, Li Y J, Qi W H and He J 2020 *Physica B* **594** 412364
[39] Tian X L, Luo H Y, Wei R F, Zhu C H, Guo Q Y, Yang D D, Wang F Q, Li J F and Qiu J R 2018 *Adv. Mater.* **30** 1801021
[40] Hurlbut W C, Lee Y S, Vodopyanov K L, Kuo P S and Fejer M M 2007 *Opt. Lett.* **32** 668
[41] Wang K P, Szydłowska B M, Wang G Z, Zhang X Y, Wang J J, Magan J J, Zhang L, Coleman J N, Wang J and Blau W J 2016 *ACS Nano* **10** 6923
[42] Demetriou G, Bookey H T, Biancalana F, Abraham E, Wang Y, Ji W and Kar A K 2016 *Opt. Express* **24** 13033
[43] Wang M X, Wang Y, Wu Y, Ma H, Jiang H, Zhao Y N, Peng Y J, Li W K, Len Y X, Yu K M and Shao J D 2024 *Adv. Funct. Mater.* **34** 2307234
[44] Huang J, Liu D Y, Chen L L, Li N, Miao L L and Zhao C J 2022 *Opt. Lett.* **47** 6413